

## Numerical simulations of the mixing potential of a high-rise inclined building

S. Cochard<sup>1</sup>, J. Paetzold<sup>1</sup>, D. F. Fletcher<sup>2</sup>, T. A. Earl<sup>1</sup>, M. K. Mohamad Khairuddi<sup>1</sup> and S. Fathieh<sup>1</sup>

<sup>1</sup>School of Civil Engineering, Faculty of Engineering and IT  
The University of Sydney, Sydney, NSW 2006, Australia

<sup>2</sup>School of Chemical and Biomedical Engineering, Faculty of Engineering and IT  
The University of Sydney, Sydney, NSW 2006, Australia

### Abstract

This paper demonstrates the efficiency of an inclined high-rise building in dispersing pollution and re-circulating fresh air to the street level of an urban neighbourhood.

### Introduction

Innovative architectural features mean that structures are subjected to complex design. The Gate of Europe in Spain, the Montreal Tower in Canada and the Schwarzwald-Baar-Center inclined tower in Germany are examples of inclined structures around the world. Current literature contains extensive wind tunnel studies and numerical simulations on vertical structures, however, flow around structures with inclination to the wind has not been thoroughly explored. Most studies on inclined structures have only focused on stay-cables (Shum et al, 2009).

This paper focuses on the impact inclined buildings can have on the flow and pollution dispersion through an urban neighbourhood (Heist et al, 2009; Brixey et al, 2009). The flow around a single building, with different tilts, was studied by numerical simulations. The results are compared against a vertical square cylinder reference building.

### Methods

To study the flow around inclined high-rise buildings, 15 different configurations were simulated using Computational Fluid Dynamics (CFD). The influence of the building tilt on the flow field was investigated by increasing the forward and sideways tilt by increments of 15° from -30° to 30°, resulting in 25 configurations. As 10 configurations out of the 25 are symmetric, they were not investigated, reducing the number of configurations studied to 15. Figure 1 shows the 15 configurations, viewed from the top, where each configuration is referred by its forward angle followed by its sideways angle, e.g. configuration -15/30 refers to a building with a backward angle of 15° and a sideways angle of 30°. Configuration 0/0 represents a vertical reference building without any tilt. In this paper, only 4 configurations are presented, for brevity; -30/0, 30/0, 0/30, and, 0/0.

To compare the CFD results with future wind tunnel investigations, 1:400 scale models were simulated rather than buildings at full scale. The 15 buildings had a square base length  $B$  of 100 mm and a vertical height  $H$  of 600 mm.

### CFD simulations

The CFD simulations modelled the University of Sydney Boundary Layer wind tunnel with high-rise inclined 100 × 100 × 600 mm buildings (Cochard et al, 2012). Even if the flow behind the buildings is governed by vortex shedding and is, by nature, unsteady, only steady-state simulations were performed at this stage as they are less CPU intensive (Hanjalić and Kenjereš, 2008).

All numerical simulations were carried out with the commer-

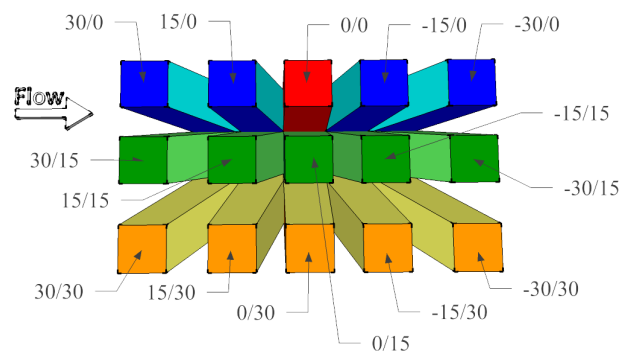


Figure 1: Sketch of the 15 configurations viewed from top. The flow is from left to right. The red building is the reference building (0/0). The blue buildings have a forward/backward tilt but no sideways tilt. The green buildings have a 15° sideways tilt. The orange buildings have a 30° sideways tilt.

cial CFD solver, ANSYS CFX 14.5 (ANSYS, 2013). CFX14.5 is based on a coupled finite volume solver for the mass and momentum (and energy if required) equations. The numerical scheme uses a collocated pressure based method and a modified Rhie-Chow algorithm to avoid decoupling (ANSYS, 2013). The resulting algebraic equations are solved by an algebraic multi-grid method. All velocity calculations use a second order bounded differencing scheme while a first order upwind scheme is implemented for the convective terms in the turbulence equations, and a second order scheme is used for all diffusive terms.

A Shear Stress Transport (SST) turbulence model was used in this work for the steady state simulations. It combines the  $k-\epsilon$  and the  $k-\omega$  models by way of a blending function (Menter, 1994). The blending function ensures that the  $k-\epsilon$  model is used in the free shear region, while the  $k-\omega$  model is used near walls, if the mesh is sufficiently fine, so the flow is resolved through the viscous sub-layer. The SST model was designed to give highly accurate predictions of the onset and the amount of flow separation under adverse pressure gradients, by the inclusion of transport effects into the formulation of the eddy-viscosity (ANSYS, 2013). This results in a major improvement in terms of flow separation predictions. The superior performance of this model has been demonstrated in a large number of validation studies (Bardina et al, 1997). The curvature correction option was activated, given that vortices are generated on the building sides.

Based on wind tunnel data, the following boundary conditions were set for the numerical simulations. A horizontal velocity boundary layer profile of  $u_{BL} = 1.3717 \cdot \ln(1658.6z + 1)$  in [m/s], where  $z$  is the height in metres, and a turbulence intensity of 0.1 were set at the inlet. The top boundary and the two lateral sides of the domain were set as free-slip walls. An average static pressure of 0Pa was set at the outlet. The building was

treated as a no-slip smooth wall, whereas the bottom boundary condition was considered as a rough wall with a sand-grain roughness of 0.018m corresponding to a physical roughness of around 0.6mm, which corresponds to the wind tunnel setup values. The fluid was air, considered incompressible and isothermal, at a temperature of 25°C.

The computational domain is shown in Figure 2 and is  $11H$  long ( $3H$  in front of the building) and  $2.5H$  high, as recommended by Revuz (2011). The employed coordinate system is:  $x$  axis orientated along the flow direction, positive towards the back of the numerical domain,  $y$  axis is orientated laterally and the  $z$  axis is vertical, positive in the upwards direction.

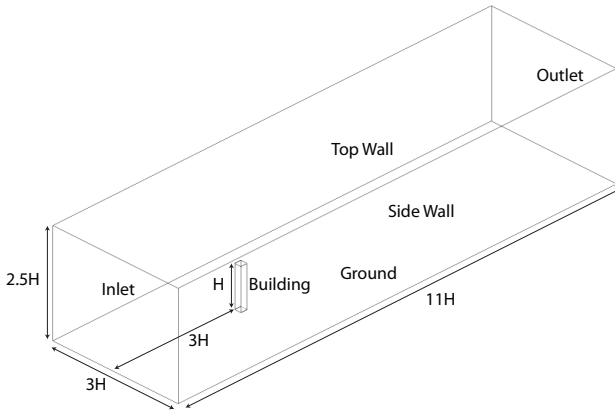


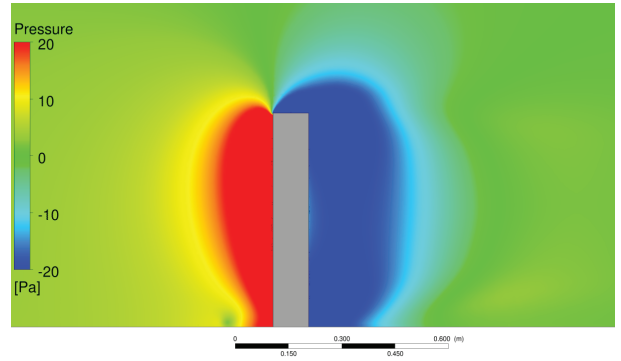
Figure 2: Sketch of the computational domain with the building located  $3H$  from the inlet.

## Results

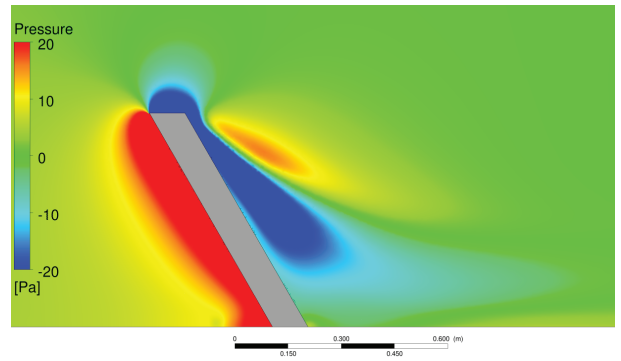
Figure 4 displays a set of 50 streamlines for each of the four configurations. For configurations 0/0, -30/0 and 0/30 (Figure 4 (a), (c) and (d) respectively), each set of streamlines starts from the bottom half of the building projection on the inlet. For configuration 30/0, the set starts at the upper half of the building projection on the inlet. The air flows from left to right and the streamlines are coloured by the velocity magnitude, from 0 m/s in blue to 12 m/s in red. If not otherwise stated, the *lower layer* refers to the lower half of the building layer, from  $z = 0$  to  $z = H/2$ , and, the *upper layer* refers to the upper half of the building, from  $z = H/2$  to  $z = H$

The flow around the reference configuration 0/0 is shown in Figure 4 (a). When the flow reaches the building it separates at its leading edges, without reattaching on its side façades, and produces two swirling vortices. The vortices detach periodically from either side of the body and generate a Von Kármán vortex street. By definition, the Von Kármán vortex street in the wake of a bluff body is a transient phenomenon and cannot be captured by a steady-state simulation.

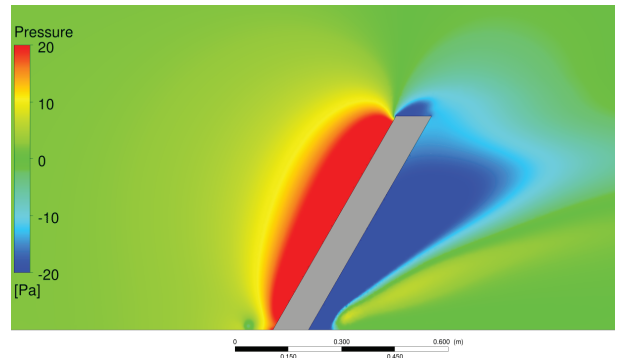
Up-washed streamlines can be observed in the near wake of the building, where a couple of streamlines travel up the downstream side of the building before being drawn back down to rejoin the majority of the lower streamlines. The near wake directly behind the building is a low pressure zone with a high level of turbulence. The streamlines fail to show the diffusion which takes place due to turbulence in the building wake. The wake region provides some mixing between the upper and the lower layer. As the building is slender, the downwash on the front façade is negligible, most of the air flows around the building. Nevertheless a stagnation point appears on the frontward



(a) Reference configuration 0/0



(b) Configuration 30/0



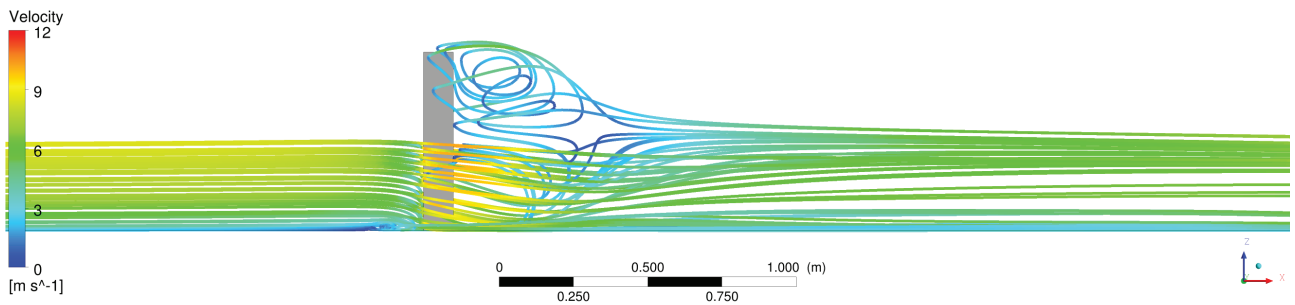
(c) Configuration -30/0

Figure 3: Pressure field around the inclined buildings, ranging from -20 Pa in blue to 20 Pa in red.

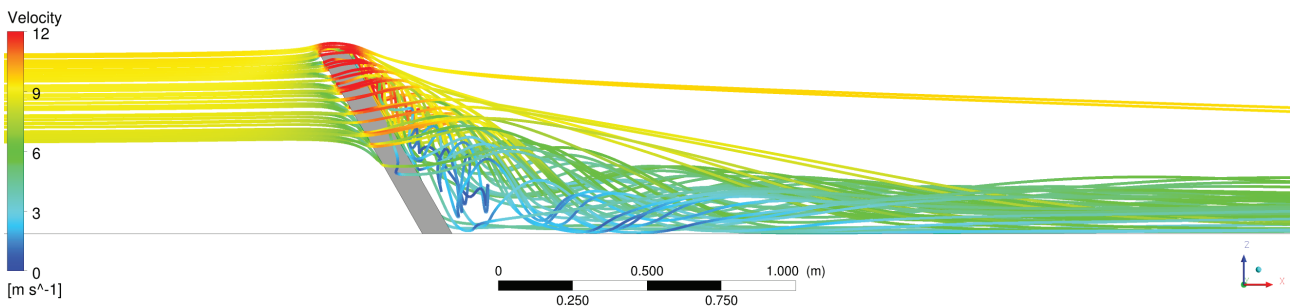
façade at  $z = 2/3 \cdot H$ , which agrees with Beranek and Koten (1979).

For the reference configuration the pressure on the front of the building increases with height  $z$  and the pressure behind the building is almost constant with  $z$  (Figure 3 (a)). The pressure increase on the front side is explained by an increase of the flow velocity up to the stagnation point at  $z = 2/3 \cdot H$ . Above  $z = 2/3 \cdot H$  the flow goes above or around the building, but not down its façade, and the pressure is reduced. The effectively constant pressure on the back can be explained by the fact the flow velocity magnitude in the near wake drops below 3 m/s.

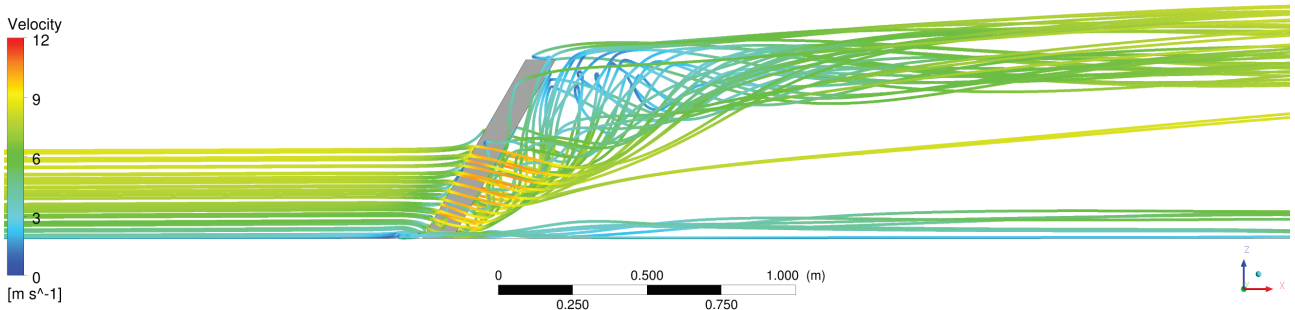
The flow around the 30° windward inclined building (30/0) is shown in Figure 4 (b). The streamlines clearly display a strong downwash flow behind the building. All streamlines, that start from the upper layer of the building projection on the inlet, end in the lower layer, except for two of them that go above the roof



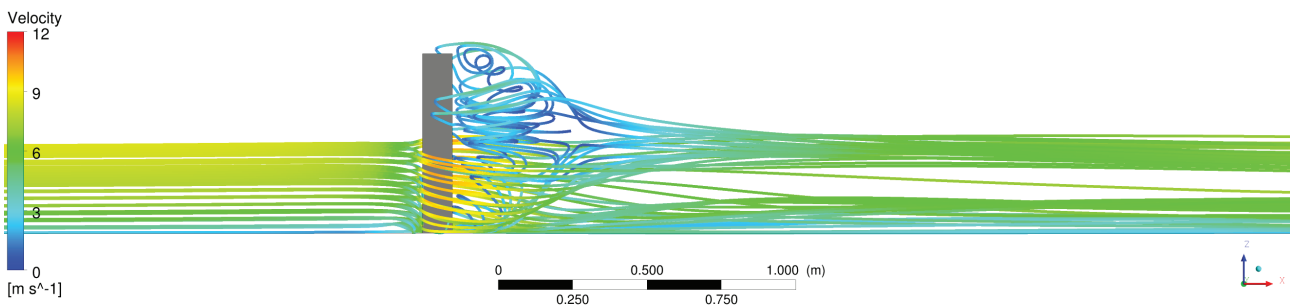
(a) Reference configuration 0/0



(b) Configuration 30/0



(c) Configuration -30/0



(d) Configuration 0/30

Figure 4: 50 streamlines coloured by the velocity magnitude, from 0 m/s in blue to 12 m/s in red. The building projection on the inlet is the starting area of the streamlines, with the lower half used for configuration 0/0 (a), -30/0 (c) and 0/30 (d), and the upper half used for configuration 30/0 (b).

of the building rather than around the sides. This configuration proves to be extremely efficient in shifting around the flow from the upper layer to the lower layer. By continuity, the same mass flux from the lower layer is moved into the upper layer, resulting in a favourable mixing regime.

The pressure distribution in the wake of configuration 30/0 is different from the reference configuration; the low pressure region behind the building on the symmetry plane  $y = 0$ , is not constant, but forms a cone, starting from the roof top, and enlarging downwards (Figure 3 (b)). The vortices that form at the building's top edges are drawn downward by the low pressure created by the lowest vortices that appear further downstream due to the building geometry. The vortices grow as they move downstream, they stay attached to the building down to  $z \approx 2/3 \cdot H$ , remain close to the building down to  $z \approx 1/3 \cdot H$  and then detached from the building before reaching the floor at  $x \approx H$ .

Figure 4 (c) shows the flow around a backwards inclined building (-30/0). The opposite flow is observed to configuration 30/0. The flow from the lower layer is moved up to the upper layer by two vortices attached to the building up to  $z \approx 2/3 \cdot H$ . The two vortices detach from the building at  $z \approx 2/3 \cdot H$  and bend to reach horizontal orientation at  $z = H$ . A couple of streamlines close to the ground are not drawn up by the building wake; they move downward as they pass the building side, 'hit' the floor and are not drawn up by the vortices.

The pressure on the back of configuration -30/0 is similar to configuration 30/0 in the sense that it forms a cone with its top on the ground and expands upward, but with one dissimilarity; the cone stays attached to the building for 2/3 of its height. The flow that is moved from the lower layer has to be replaced by flow from the upper layer which enhances the mixing process. As for configuration 30/0, configuration -30/0 is efficient in mixing the upper and lower layers.

The streamlines around configuration 0/30 are shown in Figure 4 (d), and, as for the reference configuration 0/0, do not display a strong mixing between the upper and lower layer. The mixing behind configuration 0/30 is slightly greater than for the reference configuration but is mainly due to horizontal mixing between the flow from both sides of the building.

## Discussion

The four CFD simulations presented have shown the potential for an inclined building to vertically mix the atmospheric boundary layer. Configurations 30/0 and -30/0 (Figure 4 (b), (c)), the windward and backward inclined buildings, are the most effective configurations to mix the two layers, where most of the flow from the upper, respectively lower, half of the building projection on the inlet is moved to the lower, respectively upper, half of the building height. For these two configurations the mixing process is, indeed, better than it first appears as the streamlines only shown half the flow that is mixed, the other half is made of the flow that, by continuity, is needed to fill up the void. For the sideways inclined building the mixing is far less effective than for the windward/backward configuration but better than for the reference building.

## Conclusion and future work

This study has demonstrated that an inclined high-rise building could be extremely efficient in dispersing pollution through an urban neighbourhood and bringing fresh air to the street level as long as its tilt direction is aligned with the prevailing winds. A forward or backward inclined high-rise building, relatively to the flow direction, is far more efficient to mix the wind flow

than a sidewise high-rise inclined building and a vertical one.

Future work includes;

- wind tunnel tests of the studied configurations,
- Large Eddy Simulations (LES) to capture the unsteady characteristic of the flow in the wake region and improve the estimation of the mixing capacity of an inclined high-rise buildings for different configurations,
- SST simulations inclined high-rise building with a urban neighbourhood composed of buildings of different heights.

\*

## References

- ANSYS (2013) CFX users manual. URL [www.ansys.com](http://www.ansys.com)
- Bardina J, Huang P, Coakley T (1997) Turbulence modeling validation testing and development. NASA Technical Memorandum 110446
- Beranek W, Koten HV (1979) Beperken van windhinder om gebouwen, deel 1, stichting bouwresearch no. 65. Tech. rep., Kluwer Technische Boeken BV, Deventer (in Dutch)
- Brixey L, Heist D, Richmond-Bryant J, Bowker G, Perry S, Wiener R (2009) The effect of a tall tower on flow and dispersion through a model urban neighborhood part 2. pollutant dispersion. *Journal of Environmental Monitoring* 11(2171-2179)
- Cochard S, Letchford CW, Earl TA, Montlaur A (2012) Formation of tip-vortices on prismatic-shaped cliffs. part 1: A wind tunnel study. *Journal of Wind Engineering and Industrial Aerodynamics*
- Hanjalić K, Kenjereš S (2008) Some developments in turbulence modeling for wind and environmental engineering. *Journal of Wind Engineering and Industrial Aerodynamics* 96(10-11):1537-1570
- Heist D, Brixey L, Richmond-Bryant J, Bowker G, Perry S, Wiener R (2009) The effect of a tall tower on flow and dispersion through a model urban neighborhood part 1. flow characteristics. *Journal of Environmental Monitoring* 11:2163-2170
- Menter F (1994) Two-equation eddy-viscosity turbulence models for engineering applications. *AIAA Journal* 32(8):1598-1605
- Revuz J (2011) Numerical simulation of the wind field around tall buildings and its dynamic response to wind excitation. PhD thesis, The University of Nottingham
- Shum K, PA Hitchcock P, Kwok K (2009) Galloping effects on inclined square cylinder in smooth and turbulent flows. In: The 7th Asia-Pacific Conference on Wind Engineering, Taipei, Taiwan